Title: Utilization of supercritical carbon dioxide in fabrication of cellulose acetate films with anti-biofilm effects against *Pseudomonas aeruginosa* and *Staphylococcus aureus*

Authors: Irena Zizovic, Lidija Senerovic, Ivana Moric, Tijana Adamovic, Milena Jovanovic, Melina Kalagasidis Krusic, Dusan Misic, Dusica Stojanovic, Stoja Milovanovic

PII: S0896-8446(18)30091-3
DOI: https://doi.org/10.1016/j.supflu.2018.05.025
Reference: SUPFLU 4288

To appear in: *J. of Supercritical Fluids*

Received date: 5-2-2018
Revised date: 25-5-2018
Accepted date: 25-5-2018

Please cite this article as: Zizovic I, Senerovic L, Moric I, Adamovic T, Jovanovic M, Krusic MK, Misic D, Stojanovic D, Milovanovic S, Utilization of supercritical carbon dioxide in fabrication of cellulose acetate films with anti-biofilm effects against *Pseudomonas aeruginosa* and *Staphylococcus aureus*, *The Journal of Supercritical Fluids* (2018), https://doi.org/10.1016/j.supflu.2018.05.025

Utilization of supercritical carbon dioxide in fabrication of cellulose acetate films with anti-biofilm effects against *Pseudomonas aeruginosa* and *Staphylococcus aureus*

Irena Zizovic [a*b], Lidija Senerovic[c*], Ivana Moric[c], Tijana Adamovic[d], Milena Jovanovic[a], Melina Kalagasidis Krusic[a], Dusan Misic[e], Dusica Stojanovic[a], Stoja Milovanovic[a]

[a] University of Belgrade, Faculty of Technology and Metallurgy, Karnegijeva 4, 11120 Belgrade, Serbia

[b] Wroclaw University of Science and Technology, Faculty of Chemistry, Wybrzeze Wyspianskiego 27, 50-370 Wroclaw, Poland

[c] University of Belgrade, Institute of Molecular Genetics and Genetic Engineering, Vojvode Stepe 444a, 11010 Belgrade, Serbia

[d] University of Valladolid, Department of Chemical Engineering and Environmental Technology, Valladolid – 47011, Spain

[e] University of Belgrade, Faculty of Veterinary Medicine, Bul. Oslobodjenja 18, 11000 Belgrade, Serbia

[*] Corresponding author, current address: Wroclaw University of Science and Technology, Wybrzeże S. Wyspiańskiego 27, 50-370 Wrocław, Poland, E-mail address: irena.zizovic@pwr.edu.pl

[**] Corresponding author: University of Belgrade, Institute of Molecular Genetics and Genetic Engineering, Vojvode Stepe 444a, 11010 Belgrade, Serbia, E-mail address: senerovic lidija@imgge.bg.ac.rs

Highlights

- Cellulose acetate films were impregnated with thymol using supercritical CO_2
- Target thymol contents for desired antibacterial activity were in the range 26-30%
- Thymol prevented *S. aureus* and *P. aeruginosa* attachment to films' surfaces
- Released thymol reduced biofilm formation on the surrounding surfaces
- The films showed strong anti-biofilm activity against antibiotic resistant strains

Graphical abstarct

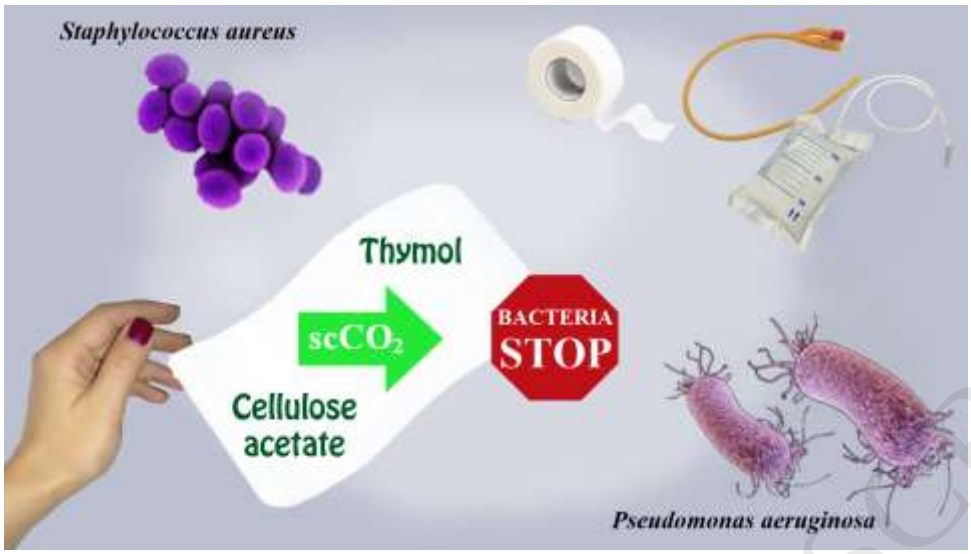

Abstract

This study discusses utilization of supercritical carbon dioxide **for** impregnation of cellulose acetate films with thymol in order to produce material with anti-biofilm activity against *Pseudomonas aeruginosa* and *Staphylococcus aureus*. Analysis of anti-biofilm activity of cellulose acetate beads impregnated with thymol suggested that optimal thymol loading was in the range from 26% to 30% for efficient reduction of biofilm formation and eradication of pre-formed biofilms. Polymer films were fabricated by the solvent casting method from polymer solutions of different contents, and loaded with thymol using supercritical carbon dioxide at 15.5 MPa and 35 ^{o}C. The film containing 30% of thymol (F1 30%) exhibited substantial anti-adhesion properties inhibiting biofilm formation on its surface and considerably reduced formation of biofilms on the surrounding surfaces (up to 80%) by all tested strains including antibiotic resistant *P. aeruginosa* DM50 and methicillin-resistant *S. aureus*.

Keywords: Supercritical carbon dioxide impregnation; *Pseudomonas aeruginosa*; *Staphylococcus aureus*; Cellulose acetate; Thymol.

1. Introduction

Supercritical carbon dioxide ($scCO_2$) has been used on the industrial scale in the extraction of valuable bioactive compounds from plant materials for decades. This green technology is particularly suitable for extraction of compounds that have low volatility and/or are susceptible to thermal degradation. Low viscosity and near zero surface tension allow $scCO_2$ to easily penetrate a solid matrix, and therefore it is also exploited in impregnation processes ensuring even distribution of an active component through the whole volume of a solid material [1].

Over the last 15 years, numerous studies on supercritical solvent impregnation (SSI) of different solid carriers with active substances using $scCO_2$ have been published. SSI with $scCO_2$ has successfully been applied on the industrial scale in wood impregnation [2-5] and textile dyeing [6-9] providing high quality products and significant reduction of pollution usually generated by these industries.

In addition, SSI has been applied to the development of materials with antibacterial activity on the laboratory scale [10-16]. Considering the urgent need for new materials with antibacterial properties, and taking into account numerous advantages of SSI**,** this technique is expected to play an essential role in their production on the industrial scale in the near future.

Antimicrobial resistance is one of the increasingly serious threats to human and animal health worldwide. In 2017 World Health Organization published a list of antibiotic-resistant "priority pathogens" – a catalogue of 12 families of multidrug resistant (MDR) bacteria that pose the greatest threat to human health, among which MDR *Pseudomonas aeruginosa* and MDR *Staphylococcus aureus* are recognized as pathogenic bacteria of critical and high priority, respectively [17].

P. aeruginosa is a major opportunistic pathogen and a common cause of hospital-acquired infections. Although healthy individuals are rarely affected with this bacterium, it can invade any part of human body and cause life-threatening diseases in patients with compromised or debilitated immune system such as in AIDS, neutropenia or severe burns. *P. aeruginosa* is involved in around 10% of all healthcare-associated infections worldwide [18].

Methicillin-resistant *S. aureus* (MRSA) causes local, purulent infections of the skin and soft tissues as well as serious systemic infections, such as osteomyelitis, necrotizing pneumonia, mastitis, and sepsis [19-21]. Due to the production of a large number of toxins and other virulence factors, MRSA strains may lead to chronic infections that often reoccur [22, 23]. In addition, biofilm-producing MRSA and methicillin-susceptible *S. aureus*, under certain conditions may cause persistent infections that cannot be cured despite the disciplined implementation of antibiotic therapy [22, 24, 25]. The lack of effective antibiotics and difficult treatments make MRSA a major challenge to modern medicine for decades.

Antimicrobial resistance occurs at two levels – the cellular level (mutation and horizontal gene transfer of resistance determinants) and bacterial community level (biofilm and persister cells). The most frequent cause of low response to antibiotic treatments in bacterial infections is the formation of biofilm. Biofilms are aggregates of microorganisms embedded in a self-produced extracellular polymeric substances (EPS) matrix that are adherent to each other and/or biotic or abiotic surface [23]. The main components of the EPS matrix are water (97%), polysaccharides, phospholipids, several proteins, and extracellular DNA [26]. Biofilm growing bacteria cause chronic infections, which are characterized by persistent inflammation and tissue damage. Some of the common human infections involving *P. aeruginosa* biofilms include

chronic cystic fibrosis pneumonia, chronic wound infections, otitis media and chronic bacterial prostatitis [27]. Beside *P. aeruginosa*, biofilms play an important role in virulence of many other pathogenic bacteria including *S. aureus, S. epidermidis* and common *Enterobacteriaceae* [28-30].

Biofilms can be formed in the patients' tissues or on the surface of medical devices associated to the human body such as catheters, naso-laryngeal tubes, or stents [29]. In a biofilm, bacteria can efficiently evade immune system and can be up to 1000-fold more resistant to antibiotics than planktonic (free-living) cells [31] due to reduced diffusion or entrapment of antibiotics by EPS matrix, slow growth rates, development of dormant persister cells, and the expression of antibiotic efflux pumps or modifying proteins [32-35]. Given the severity of biofilm infections and the limited antimicrobial arsenal for their management, finding effective strategies for biofilm prevention or dispersion is an urgent priority. One strategy for inhibition of bacterial adhesion and prevention of biofilm formation is the usage of anti-infective materials with antimicrobial or antifouling activities. The coatings and slow release of the bioactive agents can be achieved through physical adsorption, impregnation in the polymer matrix, complexation or conjugation [36].

In our previous studies [10-12] cellulose acetate (CA) was identified as a polymer suitable for SSI with thymol and its isomer carvacrol, the natural bioactive compounds with strong antibacterial properties against both Gram-positive and Gram-negative bacteria [37-39]**.** Due to the establishment of hydrogen bonds between the hydroxyl group of thymol/carvacrol and the polymer, high loadings of CA beads with these antibacterials were obtained, with up to 72% and 63% of thymol and carvacrol, respectively [10-12]. However, it was also shown that high loadings of thymol induced polymer melting due to the increased mobility of polymer chains [10]. Consequently

the question rises if it was possible to produce CA films loaded with a quantity of thymol sufficient to provide desired antibacterial activity. Potential application of such a material could be as tapes for frequently touched places in hospitals. Therefore, the aim of this study was to investigate whether SSI process could be used for the production of CA-based polymer films with anti-biofilm properties against *P. aeruginosa* and *S. aureus* strains.

2. Materials and methods

2.1. *Materials*

Thymol (purity > 99%) was purchased from Sigma-Aldrich GmbH (Steinheim, Germany). Cellulose acetate beads (CA-320S NF/EP; diameter 2.0±0.5 mm) with acetyl content of 32.0%, were a generous donation from Eastman (Kingsport, Tennessee, USA). For fabrication of CA films, acetone (Zorka, Šabac, Serbia) was used as a solvent, while glycerol (Galafarm, Skoplje, Former Yugoslav Republic of Macedonia) was used as a plasticizer in some samples. Commercial CO_2 (purity 99%) was supplied by Messer-Tehnogas (Belgrade, Serbia).

2.2. Bacterial strains and growth conditions

Pseudomonas aeruginosa PA14, *Staphylococcus aureus* ATCC 25923, *Staphylococcus aureus* ATCC 43300 (methicillin-resistant *S. aureus*), and one clinical isolate of *P. aeruginosa* DM50 with high ability to form biofilm and resistant to metronidazole, clindamycin, and amoxicillin, were used in the study. All bacterial strains were grown in Luria Bertani (LB) broth overnight (18 h) at 37 °C on a rotary shaker at 180 rpm.

2.3. Analysis of biofilm inhibitory activity of thymol impregnated cellulose acetate beads

CA beads with thymol contents of 7%, 18%, 28%, and 42% were prepared as previously described [10] and used to determine the optimal content of thymol in CA that would provide the desired anti-biofilm activity of the polymer against *P. aeruginosa* and *S. aureus* strains. The information on optimal thymol content in CA beads was used as a guideline for fabrication of thymol-impregnated CA films.

2.3.1. Quantification of biofilm formation

Biofilm quantification assay was performed in polystyrene flat base 96-well microtiter plates (Sarstedt, Germany) using a crystal violet (CV) method to stain adherent cells, with minor modifications [40]. Overnight cultures of bacteria were diluted in LB medium in order to obtain 5×10^7 colony forming units per mL (cfu mL^{-1}) and 100 µL was added to each well with a single CA bead impregnated with thymol. The number of living bacteria (cfu mL^{-1}) in the culture has been determined for each bacterial strain by serial dilutions and spread plating, according to standard procedure recommended by the Clinical and Laboratory Standards Institute (M07-A9 document) [41]. The controls of the experiments included inoculated LB containing: 1) CA beads without thymol (Ctrl*B*), 2) different concentrations of pure thymol, 2) the bacterial growth control (inoculated LB without treatment) and 3) medium sterility control (Ctrl*M*). Biofilms were allowed to form for 24 h at 37 °C and after thorough washing adhering cells were stained with CV 0.1% (v/v). After extensive washing of unbound CV with distilled water, the dye was dissolved in 30% acetic acid and the absorbance was measured at 570 nm using Tecan Infinite200 multiplate-reader (Tecan Group Ltd.,

Switzerland). Values were expressed relative to the amount of biofilm formed in the presence of CA beads without thymol according to Equation 1:

$$Biofilm\ (\%) = \frac{\mathrm{CA}th - \mathrm{Ctrl}M}{\mathrm{Ctrl}B - \mathrm{Ctrl}M} \times\ 100 \quad (1)$$

where *CAth* is measured absorbance A570 in the wells containing thymol impregnated CA beads.

Sterility of the beads was checked by incubation of the beads in LB for 24 h at 37 °C and monitoring of bacterial growth using spread plating of 50 µL from each well on LB agar. Experiments were performed in sextuplicates and repeated two times.

2.3.2. Analysis of biofilm dispersion

Overnight cultures of bacteria were diluted to 5×10^7 cfu mL^{-1} in LB, 100 µL was added per well and the plate was incubated for 24 h at 37 °C to allow biofilm formation. After removal of the supernatant and two washing steps with 200 µL sterile phosphate buffered saline (PBS), adherent cells in each well were further incubated with 100 µL fresh LB medium containing a single CA bead for additional 24 h. The controls of the experiments included: 1) sterile LB containing CA beads without thymol or 2) different concentrations of pure thymol, 3) sterile LB without treatment – bacterial growth control and 4) medium sterility control. Remaining biofilm biomass was quantified using CV method as described above. Experiments were performed two times in sextuplicates.

2.4. Fabrication of CA films

CA films were obtained by the solvent casting method. Fabricated films are presented in Table 1, where m_{CA} denotes the mass of CA dissolved in the volume of the acetone-water mixture ($V_{acetone}$ + V_{water}), with glycerol ($m_{glycerol}$) as a plasticizer or

without it. Appropriate abbreviations for the films are given according to the quantities used in the fabrication process: m_{CA} /V_{water} / $V_{acetone}$ / $m_{glycerol.}$

CA beads (0.22-1 g, Table 1) were dissolved in the acetone-water mixture (water 1.77-7.12 mL, acetone 10.68 -28 mL, Table 1) at ambient temperature of 22 ºC using magnetic stirrer during 1-3 h. Optionally, glycerol in quantity up to 38% of the CA mass (Table 1) was added at the end of the process with additional stirring for 15 min. In preliminary experiments, polymer/acetone and acetone/water ratios, as well as glycerol content, were varied. After the homogenization, the solution was poured onto a plate-like mold and left drying at ambient conditions until constant weight was achieved (3-7 days). Total volume of solution (Table 1) was around 30 mL for the most of samples, or in the range **of** 17.7-22 mL. For the 30 mL solutions, a ceramic mold of dimensions 15.5 cm x 7 cm was used. The solutions with volumes in the range 17.7-22 mL were poured onto a ceramic mold of dimensions 10 cm x 7 cm.

2.5. Supercritical solvent impregnation of CA films with thymol

The SSI of CA films with thymol was performed in a high-pressure view chamber (Eurotechnica GmbH, Germany) described in details previously [10], using the static method. Thymol (1.5 g) was placed on the bottom of the view chamber, in a glass container with a filter on its top, to avoid possible splashing during the decompression. The polymer film (2 cm x 3.5 cm) was placed in a porous basket above the thymol. After the view cell was closed and heated, $scCO_2$ was introduced into the vessel and the pressure was elevated. Based on the previous studies [10, 42], the experiments were carried out at the pressure of 15.5 MPa and temperature of 35 °C, which provided considerably high solubility of thymol in $scCO_2$ [42] and were found to be suitable for the SSI of CA beads [10]. The impregnation time was varied in the range from 2 to 32

h. Thymol was present in excess in all experiments. After each experiment, the CO_2 was released from the vessel at the rate of 1.4 MPa/min (controlled manually). The mass of impregnated thymol (m_{thymol}) was determined gravimetrically as the mass difference of the impregnated sample and sample at the beginning of the process. Thymol loading (%) of the treated CA film was calculated from Eq. 2:

$$Thymol\ loading = \frac{m_{thymol}}{m_p + m_{thymol}} \cdot 100\% \quad (2)$$

where m_p is the polymer film mass at the beginning of the process. All the experiments were performed in triplicates.

In the first experiments an influence of possible CO_2 retention in the material upon decompression was investigated. The impregnated sample was weighted half an hour after the experiment, kept in a plastic bag at 4 ^oC, and weighted again after 2h. No influence of a retained CO_2 on the calculated thymol loading (round to two decimal places) could be detected.

2.6. Analysis of anti-biofilm properties of thymol impregnated films

The effect of thymol impregnated films on the biofilm formation on the surrounding surfaces was tested in 24-well microtiter plates (Sarstedt, Germany)**.** Overnight cultures of bacteria were diluted to 5×10^7 cfu mL^{-1} in LB, and 1 mL was added to each well containing a square piece (1 cm^2) of either thymol impregnated or non-impregnated (negative control) films. The experiment controls also included the bacterial growth control (inoculated LB without films) and the medium sterility control. After incubation for 24 h at 37 °C the films were removed from the wells, planktonic cells were washed away three times with 1 mL PBS, and cells adhering to the walls of the wells were stained with CV.

In order to quantify biofilms formed on the films' surfaces, each film piece was extensively washed with sterile PBS, and adhering cells were detached into 1 mL of

PBS by sonication three times for 20 sec using ultrasonic water bath (SONIC, Ultrasonic cleaner, Serbia) at the frequency of 40 kHz [43]. Collected cells were thoroughly vortexed and ten-fold serially diluted. Appropriate dilutions were plated on LB agar plates in duplicates, and after 24 h of incubation at 37 °C formed colonies were counted. Sterility of the films was checked by incubation of the films in 1 mL LB for 24 h at 37 °C and monitoring of bacterial growth as described above**.** The experiments were performed in triplicates and the measurements were repeated three times**.**

2.7. Statistical analysis

The effects of different loading of thymol-impregnated CA beads on either biofilm formation or its disruption were analyzed by one-way ANOVA at a threshold level of $P = 0.05$, followed by the Tukey's HSD test when homogeneity of variance was met or by Games-Howell post hoc test when homogeneity was violated. All statistical analyses have been performed using SPSS 20 (SPSS Inc., Chicago, IL) software. Controls data were also included in the analysis. Statistical significance between treatment and corresponding controls have been presented in the figures with * representing $P<0.05$, while significant differences among the treatments have been described in the text.

2.8. FT-IR analysis

Fourier-transform infrared spectroscopy (FT-IR) spectra of the control CA samples (beads and film) and thymol impregnated CA film were recorded in absorbance mode using a Nicolet™ iS™ 10 FT-IR Spectrometer (Thermo Fisher Scientific, USA) with Smart iTR^{TM} Attenuated Total Reflectance (ATR) Sampling

accessories with diamond crystal, within a range of 400-4000 cm^{-1}, at a resolution of 4 cm^{-1} and in 20 scan mode.

2.9. SEM analysis

The surface morphology of CA films was analyzed by a field emission scanning electron microscopy (FESEM, Tescan Mira3 FEG, Tesacan, Brno - Kohoutovice, Czech Republic). The samples were coated with a thin layer of gold prior to analysis.

2.10. DSC analysis

Differential scanning calorimetry (DSC) analysis of the CA films was performed using a TA Instrument differential scanning calorimeter thermal analyzer (DSC Q10, TA Instruments, New Castle, USA). The samples (5-10 mg) were weighed in the aluminium pan and heated starting from the room temperature up to 300 °C at a heating rate of 10 °C/min, using nitrogen purge gas at 50 mL/min.

2.11. Thymol release kinetics

Thymol release was investigated by immersion of a sample in a physiological saline solution 9 g/L (Hemofarm, Vrsac, Serbia) at 37 ºC under static conditions. Film sample (mass 26.05 ± 0.35 mg) was immersed in 50 mL of the physiological saline solution without stirring. At pre-determined time intervals an aliquot (3 mL) of the solution was taken, analyzed and returned to the solution. Thymol concentration was determined by measuring absorption intensity at λmax=274 nm using an UV-VIS spectrophotometer Cary 100 Scan (Varian).

3. Results and discussion

3.1. Determination of optimal thymol content in CA beads and evaluation of their anti-biofilm properties

The first goal of this study was to determine thymol content in CA material necessary to efficiently establish protective effect against bacterial biofilms. The analysis had been performed with CA beads impregnated with thymol as described in our previous study [10], and the information obtained on the target thymol loadings served as a guideline for the selection of CA films due to existence of the same type of electrostatic interactions between thymol and polymer chains in both polymer morphologies. The hydroxyl group of thymol is capable of forming hydrogen bonds with functional groups of CA chains (Fig. 1) and thus interfering with intermolecular bonding between the polymer chains. Consequently, the mobility of the polymer chains is enhanced causing polymer melting at higher thymol loadings [10]. In the case of CA beads, the polymer reaches a soft melt state with thymol content of 70% [10]. According to the preliminary tests, melting of CA films occurs at lower thymol loadings compared to CA beads. Therefore, a technical problem that should be solved in the fabrication of CA films is their stability upon loading with the high quantity of thymol.

The effect of the thymol impregnated CA beads on biofilm formation by *P. aeruginosa* or *S. aureus* were tested first. In addition, although thymol is well known for its antibacterial and anti-biofilm properties, the anti-biofilm activity of the pure compound has been addressed and confirmed against bacterial strains used in this study (Supplementary data, Fig. S1). The thymol present in impregnated CA beads dose-dependently influenced biofilm formation by *P. aeruginosa* (Fig. 2 A and B**),** while CA beads without thymol did not affect formation of the biofilms (Table S1 and S2)**.** Beads containing 7% of thymol showed the stimulatory effect or no effect on biofilm

formation during 24 h and 48 h in both *P. aeruginosa* PA14 and the clinical isolate *P. aeruginosa* DM50. However, the biofilm formation was significantly reduced in both strains after 24 h or 48 h incubation with the beads containing higher amounts of impregnated thymol. After 48 h incubation with bacteria CA beads with 28% impregnated thymol allowed only 50% and 20% biofilm formation by *P. aeruginosa* PA14 ($P<0.001$) and *P. aeruginosa* DM50 ($P<0.001$), respectively. Further increase of the thymol content in CA beads showed no additional reduction of biofilm formation by *P. aeruginosa* DM50 (28% vs. 42%, $P>0.05$).

Thymol impregnated CA beads reduced biofilm formation by *S. aureus*, but the observed effect was not dependent on thymol doses (Fig. 3). When *S. aureus* ATCC 25923 strain was incubated with CA beads containing different thymol concentrations the beads containing 7% of thymol caused 45% and 60% reduction of biofilm formation after 24 h or 48 h incubation, respectively, compared to non-impregnated beads (Fig. 3A). No statistical difference has been observed between this effect and the effects observed upon incubation of bacteria with beads containing 18%, 28% or 48% of thymol either at 24 h or 48 h**.** The reduction of biofilm formation in MRSA was detected only after incubation for 48 h with thymol impregnated CA beads (Fig. 3B). Biofilm formation in MRSA was reduced to 50% in the presence of beads containing 7% of thymol and the effect was not changed by the increase of thymol concentration. Taken together, presented results indicated that thymol content of 28% provided optimal ratio between the amount of the active compound and the protective effect against biofilm formation by all tested strains.

Disruption of pre-formed biofilms is often challenging but more relevant to medical applications. Thus, whether thymol impregnated CA beads could be used for eradication of 24 hours old biofilm has been tested. Consistent with the previous

observation, 24 h incubation with the beads containing 7% of impregnated thymol stimulated growth of *P. aeruginosa* biofilms (Fig. 4). The increase of thymol content to 18% enabled eradication of *P. aeruginosa* PA14 biofilms by 30%. With further increase of thymol concentration in the beads the effectiveness of biofilm disruption was not changed (18% vs. 28%/42% for both $P>0.05$ and 28% vs. 42% $P>0.05$).

P. aeruginosa DM50 is an antibiotic resistant strain and forms thick biofilms (data not shown) that could not be disrupted with thymol impregnated CA beads, although pure compound reduced its biofilm biomass by 40% at 0.12% thymol (Fig. 4 and Supplementary data Fig. S1(D)). Interestingly, *S. aureus* ATCC 25923 biofilms could be disrupted more effectively with CA beads containing lower thymol concentration, since in the presence of impregnated beads with 7% of thymol only 50% of biofilm biomass remained on the surrounding surfaces compared to 84% of remaining biofilm biomass observed in the presence of impregnated beads with 42% of thymol (Fig. 5**;** 7% vs. 42%, $P<0.001$). On the other hand, the only statistically significant reduction of biofilm formed by MRSA has been observed in the presence of beads containing 18% of thymol (18% vs. control $P<0.01$). The pure thymol caused a similar effect with only 20% biofilm reduction when present at minimal inhibitory concentration [44-46] (MIC; Supplementary data Fig. S1(H)), indicating the low efficiency of thymol to eradicate MRSA biofilms.

Based on all results, thymol content in the range from 26% to 30% was selected as a target impregnation loading for the SSI experiments with CA films.

3.2. Selection of films for the SSI with thymol

The last column in Table 1 presents results of stability tests of films exposed to $scCO_2$ in the presence of thymol, expressed as thymol loadings when the film melting

was first observed. For each film, a set of experiments was performed under the conditions of 35 ^{o}C and 15.5 MPa for different contact times with the aim to determine a thymol loading when the film melting starts. Among the tested films, four exhibited potential for very high thymol loadings (films 4, 5, 6 and 13). Since the film No. 4 was slightly wrinkled after the solvent evaporation in the solvent casting process, films No. 5, 6, and 13 (bolded in Table 1) were finally selected for the SSI kinetics study. The selected films are named as: F1 (film No. 13 with the abbreviation 1/3/27), F2 (film No. 5 with the abbreviation 0.5/3/27) and F3 (film No. 6 with the abbreviation 0.5/3/27/0.05) in further text.

3.3. SSI of the polymer films with thymol

Kinetics of the SSI at 35 ^{o}C and 15.5 MPa for the selected films are presented in Fig. 6. Maximal thymol loadings, impregnation time, and thickness of films prior and after the SSI are given in Table 2. According to the results, the target thymol loadings set in the range from 26% to 30% can be achieved within 2 h. Therefore, processing at pressures higher than 15.5 MPa was not needed to fasten the process.

Faster impregnation was observed in the samples F2 and F3 obtained by dissolving the smaller quantity of CA (0.5 g) in the acetone-water mixture in comparison to the sample F1 obtained by dissolving the larger quantity of CA (1 g) into the same quantity of the acetone-water mixture. This could be due to the more compact structure of the film F1, which consequently brought about stronger intermolecular bonds between CA chains in F1 compared to F2 and F3. Impregnation of the films produced with the same CA mass (0.5 g) was faster at the beginning of the process when glycerol (F3) was added than when glycerol was omitted (F2). Since the film with glycerol F3 was thicker than film F2 (Table 2), this phenomenon can be attributed to

stronger intermolecular bonds and smaller distance between CA chains in the absence of glycerol (F2). The increase in thickness of the films F1 and F2 after the SSI process (Table 2) was in accordance with the previously published data on CA swelling due to the SSI with thymol [10]. In the same study, it has been shown that CA did not undergo swelling when exposed to pure $scCO_2$. Swelling occurred upon thymol interference with hydrogen bonding between the polymer chains during the SSI process [10]. On the other hand, in the case of the sample with glycerol (F3) a decrease in thickness after the SSI was detected (Table 2). Glycerol as a polar compound is poorly soluble in $scCO_2$ [47]. Therefore, a reason for the decrease in thickness could be found in complex interactions in the system thymol-CA-glycerol-$scCO_2$. To the best of our knowledge, there are no published data on the effects of glycerol in the SSI of polymers. Extensive experimental and theoretical research including molecular modeling should be performed for better understanding of this phenomenon. Additionally, the slight softening of F1 and F2 during SSI occurred at thymol loadings around 45%, causing unevenness of the films' surfaces after the decompression. However, in F3 film this effect has been observed already with loadings around 32%.

Based on these findings and previously presented results, films F1 and F2 were selected for further studies**.** A series of samples have been fabricated and following films have been selected for the evaluation of their anti-biofilm properties: F1 with 30% of thymol and F2 with 27.5% of thymol as the samples with the target thymol loadings, as well as F1 with 14% of thymol for the comparison reasons.

3.4. Anti-biofilm properties of thymol-impregnated films

Anti-biofilm properties of selected thymol-impregnated films have been tested against *P. aeruginosa* PA14. Firstly, the effects of released thymol on biofilm formation

in the wells of microtiter plates were addressed and secondly, anti-adhesion properties of the films' surfaces were analyzed (Fig. 7). Both films, F1 and F2, enabled thymol release and provided a reduction of biofilm formation on the surrounding polystyrene surface of microtiter wells. Films F1 with 30% and F2 with 27.5% thymol allowed only 20% and 18% of biofilm formation, respectively, and were more efficient than film F1 containing 14% thymol, which allowed 65% biofilm formation. All tested films demonstrated anti-adhesive properties against *P. aeruginosa* PA14 (Fig. 7) inhibiting cell attachment to the biofilm surface by 95%.

Film F1 containing 30% thymol was selected for further testing and its anti-biofilm properties were analyzed against *P. aeruginosa* DM50 and both *S. aureus* strains (Table 3). Upon incubation 24 h with bacteria the film-released thymol enabled reduction of biofilm formation on the surrounding surfaces by 32% and 50% when incubated with *S. aureus* ATCC 25923 and MRSA, respectively, while only 15% inhibition/reduction of *P. aeruginosa* DM50 biofilms was observed. Importantly, thymol impregnation significantly impaired the cell attachment to the films' surfaces for all bacterial strains tested.

These results show that SSI with thymol could protect the material surfaces from bacterial attachment and biofilm formation, as well as the material surrounding due to efficient release of the impregnated agent.

3.5. Film characterization

Pure thymol, non-impregnated CA beads and CA film F1 (control samples), and CA film F1 impregnated with 30% thymol have been analyzed by FT-IR spectroscopy. The obtained FT-IR spectra of the cellulose acetate and thymol (Figs. 8 and 9) were in accordance with the literature [48-51]. The FT-IR spectra of the beads

and the film were identical, except for small difference noticed in the range 2926-2857 cm^{-1}. An additional band at 2857 cm^{-1}, observed in the spectra of CA film, is attributed to C-H bending [51].

Besides the bands that are characteristic for cellulose acetate, the FT-IR spectrum of CA film impregnated with thymol revealed additional absorption bands which are characteristic for thymol (Fig. 9c) [52-54], where the intensity of the absorption bands was changed and slightly shifted to lower or higher wavenumbers. The bands at 2960 cm^{-1} and 2874 cm^{-1} are assigned to methyl group [55-57], while those at 1618 and 1458 cm^{-1} correspond to phenol ring of thymol [52, 54]. The peaks related to ring vibration of thymol [53, 57] were detected in the spectrum at 947 cm^{-1}, 811 cm^{-1} and 736 cm^{-1}. The observed bands confirmed that thymol has been successfully incorporated into the film without chemical modification. In addition, the main change observed for –OH stretching peak at 3181 cm^{-1} might indicate interaction of thymol with cellulose acetate via hydrogen bonds.

SEM images of films F1 and F2 before and after the SSI are presented in Fig. 10. No significant change can be observed in the films' morphology upon loadings with the target thymol contents (30% for F1 and 26% for F2). However, results of the DSC analysis presented in Fig. 11 revealed strong plasticizing effect of thymol. The thermograms of film F1 samples before the SSI (control) and with 30% of thymol are presented in Fig. 11. The first broad endothermic peaks located at ~100 ºC and ~89 ºC for the control (a) and impregnated sample (b) respectively, are attributed to the evaporation of the remained water and plasticizer used for the fabrication of polymer [58]. The thermograms indicated important effects of thymol on the glass transition temperature (T_g). The control sample is characterized by a T_g at 221.7 ºC. The addition of 30 wt.% of thymol to film F1 resulted in a decrease of the Tg value for approximately

35 ºC. Likewise, the endothermic peak of the control sample which exists at 246.9 °C was shifted to lower temperature of 220.7 °C for the impregnated sample, indicating decrease in the melting temperature. At the same time, the change in the sample melting enthalpy from 4.2 J/g (control) to 0.68 J/g (impregnated sample) pointed out a decrease in the crystallinity of the impregnated sample. The decomposition of the sample with 30% of thymol started at a temperature above 240 ºC.

Thymol release from the film F1 sample with 30% of thymol was investigated in a physiological saline in order to simulate the body fluids. The kinetics of thymol release is presented in Fig. 12. The film released around 90% of the impregnated thymol after 360 min, and around 70% in the first 120 min. Bearing in mind that one of the possible applications of CA films impregnated with thymol could be in wound dressings, aforesaid release kinetics might be desirable

4. Conclusion

Results of this study demonstrated efficient utilization of SSI for the fabrication of cellulose acetate based films with anti-biofilm properties against *P. aeruginosa* and *S. aureus*. Film F1 with 30% of thymol, obtained by the SSI at 15.5 MPa and 35 ºC, showed excellent anti-biofilm activity ensuring protection from bacterial attachment to the films' surfaces for all tested strains. The release of the thymol from the film also reduced biofilm formation on the surrounding surfaces.

The cellulose acetate films subjected to the SSI in this study were produced on the laboratory scale by the solvent casting method. In the medical device industry, the solvent casting method is applied for the production of flexible plastic components such as catheters. However, many cellulose acetate forms that could be utilized in the hospitals at places of high risk for biofilm formation are commonly produced by the

extrusion method due to the lower price and easier process control. Based on the results presented in this study, the next step could be the application of the SSI process for the bioactivity enhancement of cellulose acetate films obtained by the extrusion process.

Acknowledgments

Financial support of the Serbian Ministry of Education, Science and Technological Development (Projects III45017 and OI173048) is gratefully acknowledged.

References

[1] C. Wolf, J. Maninger, K. Lederer, H. Fruhwirth-Smounig, T. Gamse, R. Marr, Stabilisation of crosslinked ultra-high molecular weight polyethylene (UHMW-PE)-acetabular components with α-tocopherol, J. Mater. Sci.: Mater. Med. 17 (2006) 1323–1331. doi: 10.1007/s10856-006-0607-7.

[2] O. Henriksen, Method of performing an impregnating or extracting treatment on a resin-containing wood substrate, US Patent 6,517,907 B1 (2003).

[3] O. Henriksen, Method of performing an impregnating or extracting treatment on a resin-containing wood substrate, US Patent 6,623,600 B1 (2003).

[4] A. Qader, Wood preservation, US Patent 6,638,574 B1 (2003).

[5] A.W. Kiellow, O. Henriksen, Supercritical wood impregnation, J. of Supercritical Fluids 50 (2009) 297-304.

[6] DyeCoo, http://www.dyecoo.com (14.08.2017).

[7] M.V.F. Cid, G.J. Witkamp, G.F. Woerlee, W.J.T. Veugelers, Method of dyeing a substrate with a reactive dyestuff in supercritical or near supercritical carbon dioxide, US Patent 7,731,763 B2 (2010).

[8] W. Schlenker, P. Liechti, D. Werthemann, A.D. Casa, Process for dyeing cellulosic textile material with disperse dyes, US Patent 5,298,032 (1994).

[9] W. Saus, D.K. Grevenbroich, E.S. Krefeld, H.J.B. Kempen, Process for dyeing hydrophobic textile material with disperse dyes from supercritical CO2 : reducing the pressure in stages, US Patent 5,250,078 (1993).

[10] S. Milovanovic, M. Stamenic, D. Markovic, J. Ivanovic, I. Zizovic, Supercritical impregnation of cellulose acetate with thymol, J. of Supercritical Fluids 97 (2015) 107-115.

[11] S. Milovanovic, D. Markovic, K. Aksentijevic, D. B. Stojanovic, J. Ivanovic, I. Zizovic, Application of cellulose acetate for controlled release of thymol, Carbohydrate Polymers 147 (2016) 344-353.

[12] S. Milovanovic, T. Adamovic, K. Aksentijevic, D. Misic, J. Ivanovic, I. Zizovic, International Journal of Polymer Science, Cellulose Acetate Based Material with Antibacterial Properties Created by Supercritical Solvent Impregnation, 2017 (2017) Article ID 8762649, 9 pages. https://doi.org/10.1155/2017/8762649

[13] Y. Chen, P. Yu, C. Feng, Y. Wang, Q. Han, Q. Zhang, Synthesis of polysiloxane with quaternized N-halamine moieties for antibacterial coating of polypropylene via supercritical impregnation technique, Applied Surface Science 419 (2017) 683-691.

[14] J. Sanchez-Sanchez, M.T. Fernández-Ponce, L. Casas, C. Mantell, E.J. Martínez de la Ossa, Impregnation of mango leaf extract into a polyester textile using supercritical carbon dioxide, J. of Supercritical Fluids 128 (2017) 208-217.

[15] N. Mölders, M. Renner, C. Errenst, E. Weidner, Incorporation of antibacterial active additives inside polycarbonate surfaces by using compressed carbon dioxide as transport aid, J. of Supercritical Fluids 132 (2018) 83-90.

[16] M.A. Fanovich, J. Ivanovic, D. Misic, M.V. Alvarez, P. Jaeger, I. Zizovic, R. Eggers, Development of polycaprolactone scaffold with antibacterial activity by an integrated supercritical extraction and impregnation process, J. of Supercritical Fluids 78 (2013) 42-53.

[17] Prioritization of pathogens to guide discovery, research and development of new antibiotics for drug-resistant bacterial infections, including tuberculosis. Geneva: World Health Organization; 2017(WHO/EMP/IAU/2017.12)

[18] V. Aloush, S. Navon-Venezia, Y. Seigman-Igra, S. Cabili, Y. Carmeli, Multidrug-Resistant Pseudomonas aeruginosa: Risk Factors and Clinical Impact, Antimicrobial Agents and Chemotherapy 50 (2006) 43-48.

[19] T.Chua, C.L. Moore, M.B. Perri, , S.M. Donabedian, , W. Masch, , D. Vager, S.L. Davis, K. Lulek, B. Zimnicki, M.J. Zervos, Molecular Epidemiology of Methicillin-Resistant Staphylococcus aureus Bloodstream Isolates in Urban Detroit, J. of Clinical Microbiology 46 (2008) 2345–2352.

[20] F.X. Lescure, G. Locher, M. Eveillard, M. Biendo, S. Van Agt, G. Le Loup, Y. Douadi, O. Ganry, F. Vandenesch, F. Eb, J.L. Schmit, J. Etienne, Community-Acquired Infection With Healthcare-Associated Methicillin-Resistant Staphylococcus aureus: The Role of Home Nursing Care, Infection Control & Hospital Epidemiology 27 (2006) 1213–1218.

[21] B. Suvajdžić, V. Teodorović, D. Vasilev, N. Karabasil, M. Dimitrijević, J. Đorđević, V. Katić, Detection of icaA and icaD genes of *Staphylococcus aureus* isolated in cases of bovine mastitis in the Republic of Serbia, Acta Veterinaria 67 (2017) 168-177.

[22] J.O. Cha, J.I. Yoo, J.S. Yoo, H.S. Chung, S.H. Park, H.S. Kim, Y.S. Lee, G.T. Chung, Investigation of Biofilm Formation and its Association with the Molecular and

Clinical Characteristics of Methicillin-resistant Staphylococcus aureus, Osong Public Health and Research Perspectives 4 (2013), 225-232.

[23] H.C. Flemming, J. Wingender, U. Szewzyk, P. Steinberg, S.A. Rice, S.F. Kjelleberg, Biofilms: an emergent form of bacterial life, Nature Reviews Microbiology 14 (2016) 563-575.

[24] H. McCarthy, J.K.Rudkin, N.S. Black, L. Gallagher, E. O'Neill, J.P. O'Gara, Methicillin resistance and the biofilm phenotype in *Staphylococcus aureus*, Frontiers in Cellular and infection Microbiology 5 (2015) 1-9.

[25] E. O'Neill, C. Pozzi, P. Houston, D. Smyth, H. Humphreys, D.A. Robinson, J.P. O'Gara , Association between Methicillin Susceptibility and Biofilm Regulation in Staphylococcus aureus Isolates from Device-Related Infections, J. of Clinical Microbiology 45 (2007) 1379-1388.

[26] H.C. Flemming, J. Wingender, The biofilm matrix, Nature Reviews Microbiology 8 (2010) 623-633.

[27] J.B. Lyczak, C.L. Cannon, G.B. Pier, Establishment of Pseudomonas aeruginosa infection: lessons from a versatile opportunist, Microbes and Infection 2 (2000) 1051-1060.

[28] J.W. Costerton, P.S. Stewart, E.P. Greenberg, Bacterial biofilms: a common cause of persistent infections, Science 284 (1999) 1318-1322.

[29] J.D. Bryers, Medical Biofilms, Biotechnology and Bioengineering 100 (2008) 1-18.

[30] P.K. Singh, A.L. Schaefer, M.R. Parsek, T.O. Moninger, M.J. Welsh, E.P. Greenberg, Quorum-sensing signals indicate that cystic fibrosis lungs are infected with bacterial biofilms, Nature 407 (2000) 762-764.

[31] Y. Oppenheimer-Shaanan, N. Steinberg, I. Kolodkin-Gal, Small molecules are natural triggers for the disassembly of biofilms, Trends in Microbiology 21 (2013) 594-601.

[32] N. Bagge, M. Schuster, M. Hentzer, O. Ciofu, M. Givskov, E.P. Greenberg, N. Høiby, *Pseudomonas aeruginosa* Biofilms Exposed to Imipenem Exhibit Changes in Global Gene Expression and β-Lactamase and Alginate Production, Antimicrobial Agents and Chemotherapy 48 (2004) 1175-1187.

[33] T.F. Mah, B. Pitts, B. Pellock, G.C. Walker, P.S. Stewart, G.A. O'Toole, A genetic basis for *Pseudomonas aeruginosa* biofilm antibiotic resistance, Nature 426 (2003) 306-310.

[34] B.D. Hoyle, J. Alcantara, J.W. Costerton, Pseudomonas aeruginosa biofilm as a diffusion barrier to piperacillin, Antimicrobial Agents and Chemotherapy 36 (1992) 2054-2056.

[35] G.V. Tetz, N.K. Artemenko, V.V. Tetz, Effect of DNase and Antibiotics on Biofilm Characteristics, Antimicrobial Agents and Chemotherapy 53 (2009) 1204-1209.

[36] I. Francolini, C. Vuotto, A. Piozzi, G. Donelli, Antifouling and antimicrobial biomaterials: an overview, Acta Pathologica, Microbiologica, et Immunologica Scandinavica 125 (2017) 392-417.

[37] A. Wattanasatcha, S. Rengpipat, S. Wanichwecharungruang, Thymol nanospheres as an effective anti-bacterial agent, International Journal of Pharmaceutics 434 (2012) 360-365.

[38] S. Cosentino, C.I. Tuberoso, B. Pisano, M. Satta, V. Mascia, E. Arzedi, F. Palmas, *In-vitro* antimicrobial activity and chemical composition of Sardinian *Thymus* essential oils, Letters in Applied Microbiology 29 (1999) 130-135.

[39] A. Nostro, A.R. Blanco, M. A Cannatelli, V. Enea, G. Flamini, I. Morelli, A. S. Roccaro, V. Alonzo, Susceptibility of methicillin-resistant staphylococci to oregano essential oil, carvacrol and thymol, FEMS Microbiology Letters 230 (2004) 191–195.

[40] J.H. Merritt, D. E. Kadouri, G. A. O'Toole, Growing and Analyzing Static Biofilms, Current Protocol in Microbiology (2005) 1B.1.1–1B.1.17.

[41] Clinical and Laboratory Standards Institute (2012). M07-A9. Methods for dilutionantimicrobial susceptibility tests for bacteria that grow aerobically; Approved standard: 9th ed. CLSI, W.P.

[42] S. Milovanovic, M. Stamenic, D. Markovic, M. Radetic, I. Zizovic, Solubility of thymol in supercritical carbon dioxide and its impregnation on cotton gauze, J. of Supercritical Fluids 84 (2013) 173-181.

[43] A.Assere, N. Oulahal, B. Carpentier, Comparative evaluation of methods for counting surviving biofilm cells adhering to a polyvinyl chloride surface exposed to chlorine or drying, J. of Applid Microbiology 104 (2008) 1692-1702.

[44] D. Kifer, V. Muzinic, M.S. Klaric, Antimicrobial potency of single and combined mupirocin and monoterpenes, thymol, menthol and 1,8-cineole against Staphylococcus aureus planktonic and biofilm growth, Journal of Antibiotics (Tokyo) 69 (2016) 689-696.

[45] A. Nostro, A.R. Blanco, M.A. Cannatelli, V. Enea, G. Flamini, I. Morelli, A. Sudano Roccaro, V. Alonzo, Susceptibility of methicillin-resistant staphylococci to oregano essential oil, carvacrol and thymol, FEMS Microbiology Letters 230 (2004) 191-195.

[46] M. Sokovic, J. Glamoclija, P.D. Marin, D. Brkic, L.J. van Griensven, Antibacterial effects of the essential oils of commonly consumed medicinal herbs using an in vitro model, Molecules 15 (2010) 7532-7546

[47] H. Sovova, J. Jez, M. Khachaturyan, Solubility of squalane, dinonyl phthalate and glycerol in supercritical CO_2, Fluid Phase Equilibria 137 (1997) 185-191.

[48] S. Waheed, A. Ahmad, S.M. Khan, S. Gul, T. Jamil, A. Islam, T. Hussain, Synthesis, characterization, permeation and antibacterial properties of cellulose acetate/polyethylene glycol membranes modified with chitosan, Desalination 351 (2014) 59-69.

[49] C. Liu, R. Bai, Preparation of chitosan/cellulose acetate blend hollow fibers for adsorptive performance, J. of Membrane Science 267 (2005) 68-77.

[50] A. Khalf, K. Singarpu, S.V. Madihally, Cellulose acetate core–shell structured electrospun fiber: fabrication and characterization, Cellulose 22 (2015) 1389-1400.

[51] F.S. Dehkordi, M. Pakizeh, M.N. Mahboub, Properties and ultrafiltration efficiency of cellulose acetate/organically modified Mt (CA/OMMt) nanocomposite membrane for humic acid removal, Applied Clay Science 105-106 (2015) 178-185.

[52] M. K. Trivedi, S. Patil, R. K. Mishra, S. Jana, Structural and Physical Properties of Biofield Treated Thymol and Menthol, J. of Molecular Pharmaceutics & Organic Process Research 3 (2015) 127. doi: 10.4172/2329-9053.1000127.

[53] D. Markovic, S. Milovanovic, M.Radetic, B. Jokic, I. Zizovic, Impregnation of corona modified polypropylene non-woven material with thymol in supercritical carbon dioxide for antimicrobial application, J. of Supercritical Fluids 101 (2015) 215-221.

[54] M.J. Mohammed, F.A. al-Bayati, Isolation and identification of antibacterial compounds from Thymus kotschyanus aerial parts and Dianthus caryophyllus flower buds, Phytomedicine 16 (2009) 632-637.

[55] A. Pozefsky, N. D. Coggeshall, Infrared Absorption Studies of Carbon-Hydrogen Stretching Frequencies in Sulfurized and Oxygenated Materials, Analytical Chemistry 23 (1951) 1611-1619.

[56] C.M. Topala, L.D. Tataru, ATR-FTIR Study of Thyme and Rosemary Oils Extracted by Supercritical Carbon Dioxide, Revista de Chimie –Bucharest 67 (2016) 842-846.

[57] I.S. Al-Sheibany, Qualitative and Quantitative Evaluation of some Organic Compounds in Iraqi Thyme, Iraqi National J. of Chemistry 19 (2005) 366-379.

[58] J. Pajnik, M. Radetić, D. B. Stojanovic, I. Jankovic-Častvan, V. Tadic, M. V. Stanković, D. M. Jovanović, I. Zizovic, Functionalization of polypropylene, polyamide and cellulose acetate materials with pyrethrum extract as a natural repellent in supercritical carbon dioxide, J. of Supercritical Fluids 136 (2018) 70-81.

Figure captions

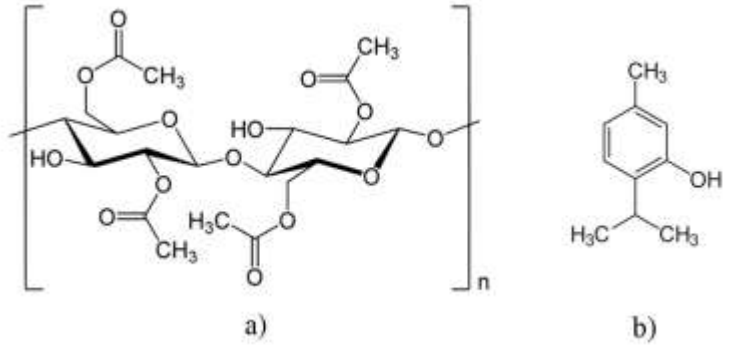

Fig. 1. Structural formulas of cellulose acetate (a) and thymol (b).

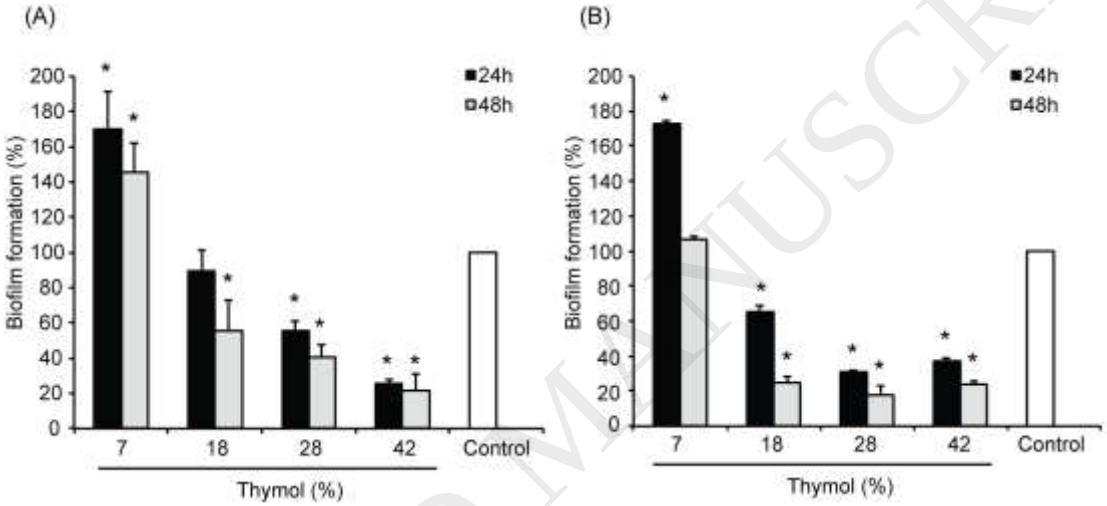

Fig. 2. Effects of thymol-impregnated beads on biofilm formation in (A) *P. aeruginosa* PA14 and (B) clinical strain *P. aeruginosa* DM50, after 24 h and 48 h incubation with thymol impregnated beads. Controls represent biofilm formation in the presence of non-impregnated beads (100%). Values are representative of two independent experiments performed in sextuplicates, presented as mean ± SD. *P<0.05.

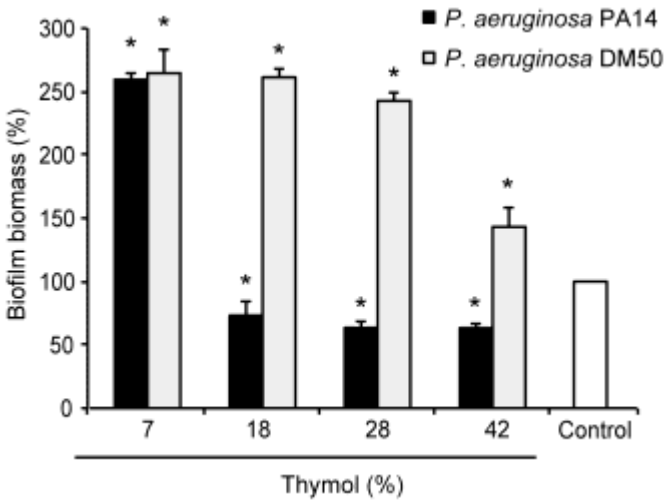

Fig. 3. Effects of thymol-impregnated beads on biofilm formation in (A) *S. aureus* ATCC 25923 and (B) *S. aureus* ATCC 43300 MRSA, after 24 h and 48 h incubation with thymol impregnated beads. Controls represent biofilm formation in the presence of non-impregnated beads (100%). Values are representative of two independent experiments performed in sextuplicates, presented as mean ± SD. *P<0.05.

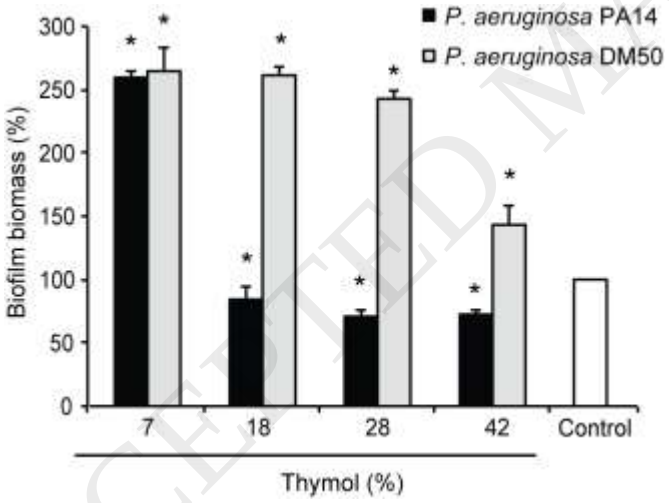

Fig. 4. Effects of thymol-impregnated beads on the biomass of pre-formed *P. aeruginosa* biofilms in the presence of thymol impregnated beads. Controls represent biofilm formation in the presence of non-impregnated beads (100%). Values are representative of two independent experiments performed in sextuplicates, presented as mean ± SD. *P<0.05.

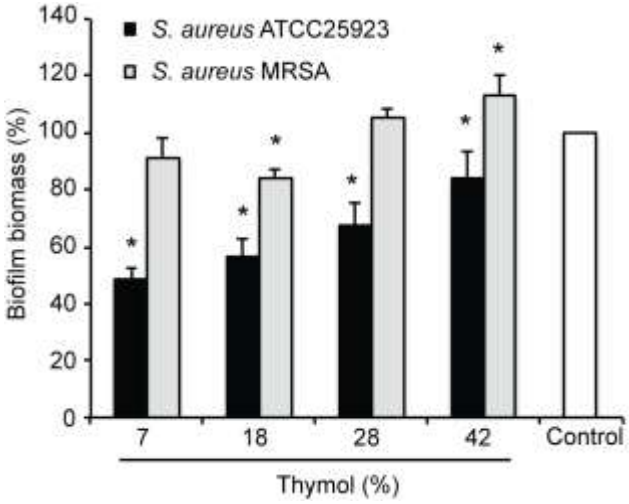

Fig. 5. Effects of thymol-impregnated beads on the biomass pre-formed *S. aureus* biofilms. Controls represent biofilm formation in the presence of non-impregnated beads (100%). Values are representative of two independent experiments performed in sextuplicates, presented as mean ± SD. *P<0.05.

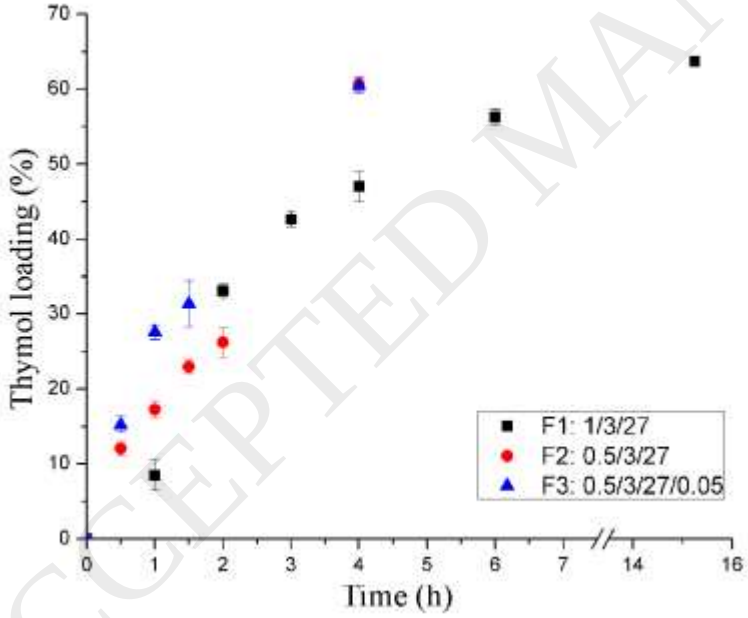

Fig. 6. SSI kinetics for the selected films at 35 ºC and 15.5 MPa.

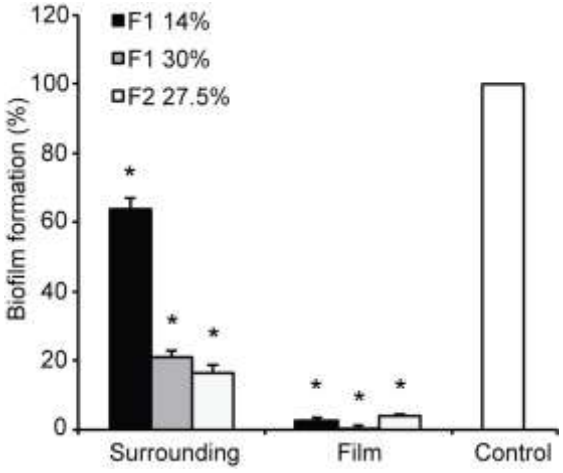

Fig. 7. Inhibition of *P. aeruginosa* PA14 biofilm formation on the bottom of the wells in polystyrene plate (surrounding) and on the surface of thymol-impregnated films (film). Controls represent biofilm formation in the presence of non-impregnated films (100%). Values are representative of three independent experiments performed in triplicates, presented as mean ± SD. *P<0.05**.**

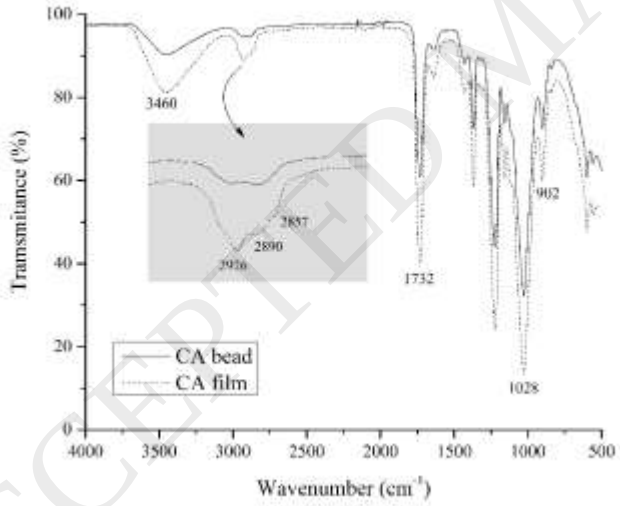

Fig. 8. FT-IR spectra of CA bead and CA film F1 (control samples).

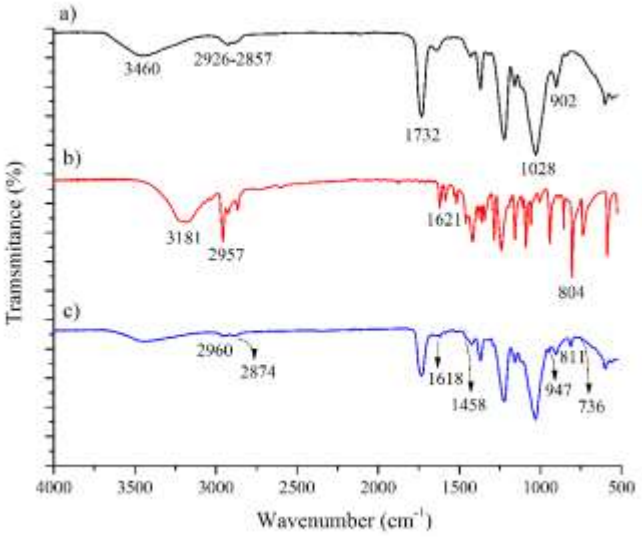

Fig. 9. FT-IR spectra of: a) CA film F1 (control), b) thymol, c) CA film F1 with 30% of thymol.

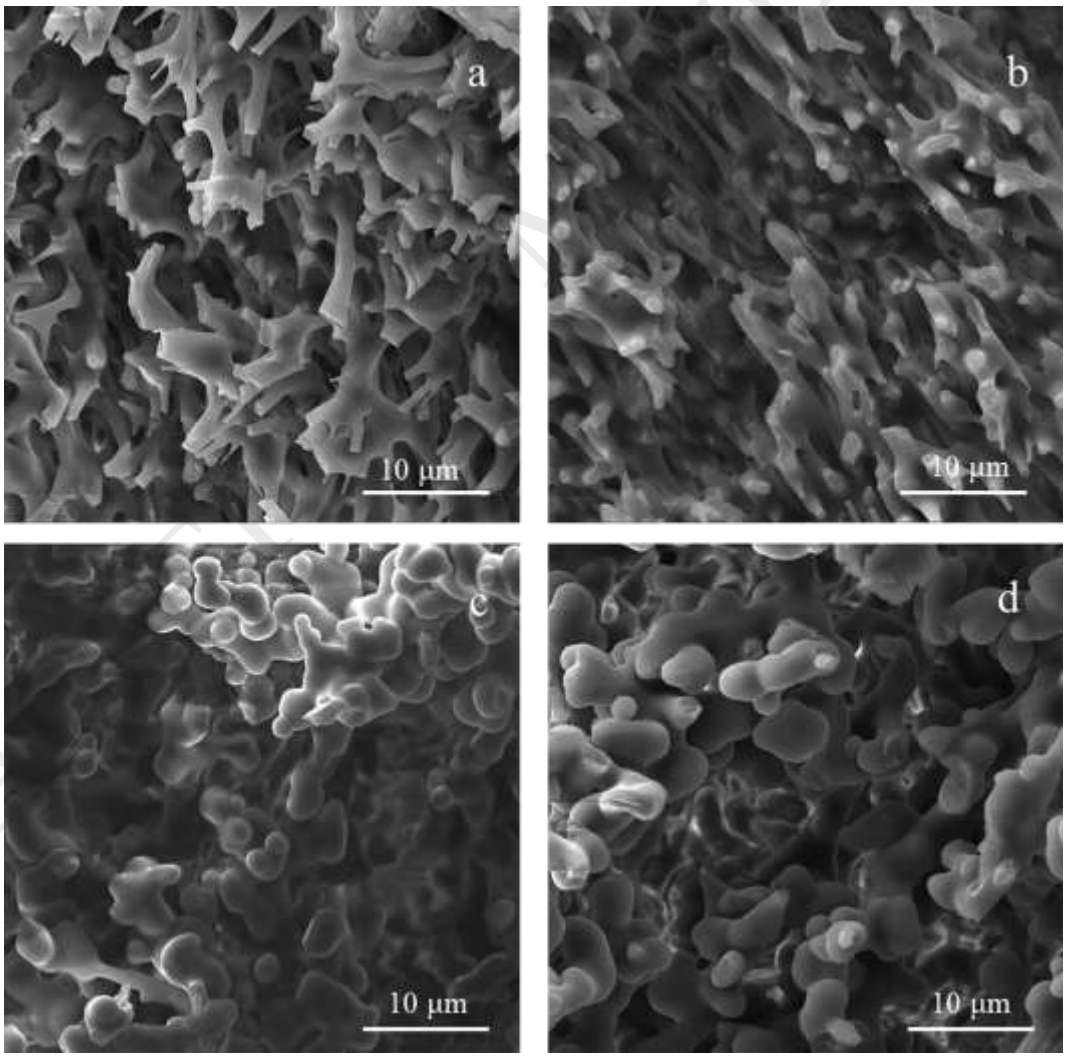

Fig. 10. SEM images of CA films: a) control F1; b) F1 with 30% of thymol; c) control F2; d) F2 with 26% of thymol.

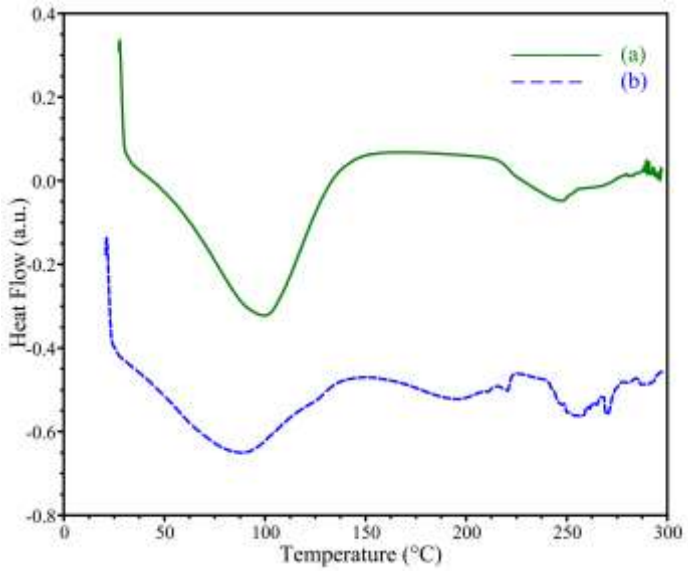

Fig. 11. DSC thermograms of the control F1 sample (a) and F1 sample with 30% of thymol (b).

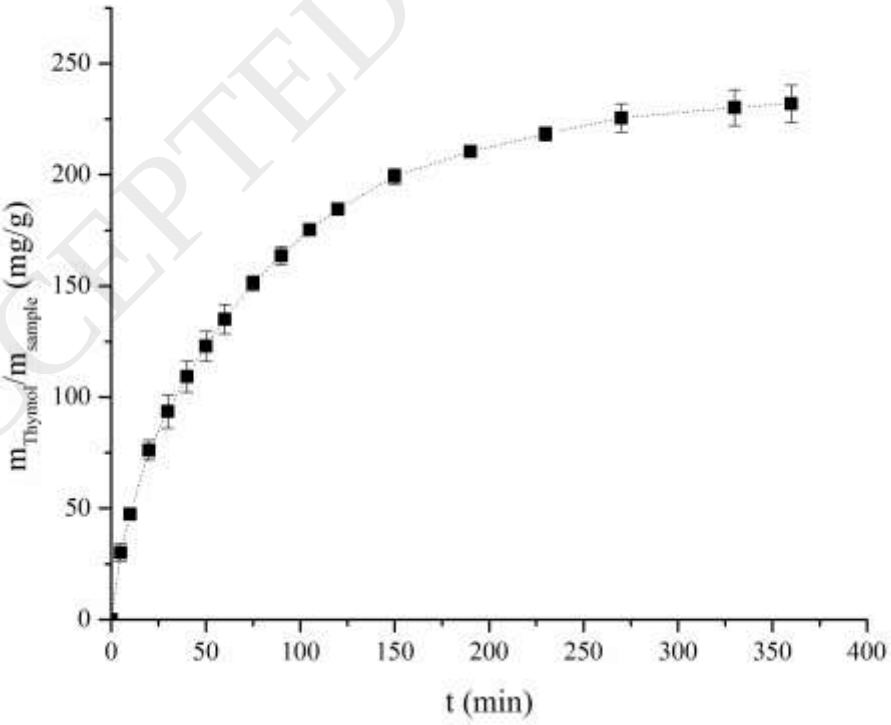

Fig. 12. Mass of thymol released per mass of the impregnated F1 film with 30% of thymol in physiological saline solution.

Tables

Table 1. List of fabricated CA films and thymol loadings when melting was **observed.**

No.	m_{CA} [g]	V_{water} [mL]	$V_{acetone}$ [mL]	$m_{glycerol}$ [g]	Film abbreviation	Thymol loading (%)
1.	0.5	2	28	0	0.5/ 2/ 28	29
2.	1.0	2	28	0	1/ 2/ 28	42.5
3.	0.25	3	27	0	0.25/ 3/ 27	22.3
4.	0.22	2.2	19.8	0	0.22/ 2.2/ 19. 8	62.3*
5.	**0.5**	**3**	**27**	**0**	**0.5/ 3/ 27**	**61.2**
6.	**0.5**	**3**	**27**	**0.05**	**0.5/ 3/ 27/ 0.05**	**55.1**
7.	0.5	2	18	0	0.5/ 2/ 18	18.5
8.	0.8	3	27	0	0.8/ 3/ 27	**
9.	0.8	3	27	0.27	0.8/ 3/ 27/ 0.27	**
10.	0.47	1.77	15.93	0.181	0.47/ 1.77/ 15.93/ 0.181	8.8
11.	0.66	2.2	19.8	0	0.66/ 2.2/ 19.8	4.1
12.	0.66	2.2	19.8	0.225	0.66/ 2.2/ 19.8/ 0.225	23.9
13.	**1.0**	**3**	**27**	**0**	**1/ 3/ 27**	**64.1**
14.	0.59	1.78	16	0.039	0.593/ 1,78/ 16/ 0,039	44.9
15.	1.0	3	27	0.1	1/ 3/ 27/ 0,1	50.7
16.	1.0	3	27	0.264	1/ 3/ 27/ 0,264	46.4
17.	1.1	3	27	0	1.1/ 3/ 27/ 0	34.7
18.	0.65	1.78	16.02	0.244	0.65/ 1.78/ 16.02/ 0.244	48.5
19.	1	2	18	0	1.0/ 2 /18	36.2
20.	0.59	3.56	14.24	0	0.59/ 3.56/ 14.24	33.6
21.	0.59	7.12	10.68	0	0.59/ 7.12/ 10.68	**
22.	0.59	7.12	10.68	0.211	0.59/ 7.12/ 10.68/ 0.211	24.6

* - the film was wrinkled upon fabrication (prior to the SSI)

** - the film was brittle upon fabrication (prior to the SSI) and was not taken into consideration for the SSI

Table 2. Thymol loadings given as mean values from triplicates for the selected films

Film	I_{max} (%)	Impregnation time (h)	Initial thickness (mm)	Thickness after SSI*(mm)
F1	63.7±0.6	15.4	0.19 ±0 .0089	0.23±0.034
F2	60.6±0.9	4	0.12 ± 0.012	0.16±0.012
F3	60.4±0.9**	4	0.16 ± 0.0082	0.14±0.025

*Thymol loadings in F1 and F2 around 60%; Thymol loading in F3: 34.7% (because of the film unevenness with larger thymol loadings)

**The film was partially melted which is in accordance with the data from Table 1

Table 3. Inhibition of biofilm formation on the bottom of the wells in polystyrene plates (surrounding) and cell adhesion on the surface of thymol-impregnated films (F1 30%). Values are presented as mean ± SD.

Pathogen	**Surrounding** (inhibition of biofilm formation %)	**Cell adhesion on films** (cell count)	
		Control (10^7)	with thymol (10^3)
P. aeruginosa PA14	79±1.5	1.4±0.7	0.7±0.6
P. aeruginosa DM50	15±1.5	20±1.0	7.5±1.5
S. aureus ATCC 25923	32±4	1.1±0.6	0
MRSA	50±0.5	1.5±1.0	0